Extreme dark matter tests with extreme mass ratio inspirals

Otto A. Hannuksela,[1,2,*] Kenny C. Y. Ng,[3,†] and Tjonnie G. F. Li[4,‡]

[1]*Institute for Gravitational and Subatomic Physics (GRASP), Department of Physics, Utrecht University, Princetonplein 1, 3584 CC Utrecht, The Netherlands*
[2]*Nikhef—National Institute for Subatomic Physics, 105 Science Park, 1098 XG Amsterdam, Netherlands*
[3]*Department of Particle Physics and Astrophysics, The Weizmann Institute of Science, Rehovot 76100, Israel*
[4]*Department of Physics, The Chinese University of Hong Kong, Sha Tin, N.T., Hong Kong*

(Received 24 October 2019; accepted 16 October 2020; published 19 November 2020)

Future space-based laser interferometry experiments such as LISA are expected to detect $\mathcal{O}(100–1000)$ stellar-mass compact objects falling into massive black holes in the centers of galaxies, the so-called extreme-mass-ratio inspirals (EMRIs). If dark matter forms a "spike" due to the growth of the massive black hole, it will induce a gravitational drag on the inspiralling object, changing the EMRI orbit and gravitational-wave signal. We show that detection of even a single dark matter spike from an EMRI will severely constrain several popular dark matter candidates, such as ultralight bosons, keV fermions, MeV–TeV self-annihilating dark matter, and sub-solar mass primordial black holes, as these candidates would flatten the spikes through various mechanisms. Future space gravitational wave experiments could thus have a significant impact on the particle identification of dark matter.

DOI: 10.1103/PhysRevD.102.103022

I. INTRODUCTION

Astrophysical and cosmological observations from vastly different scales have established the existence of nonbaryonic substance—dark matter (DM)—that makes up around 85% of all known matter [1,2]. Significant effort has gone into identifying DM, whose discovery will be a crucial breakthrough in fundamental physics and understandings of the Universe.

Many probes of DM utilize regions of high DM densities, such as the Galactic halo and dwarf spheroidals (dSphs). One attractive target for such searches is the DM spikes, dense concentrations of DM surrounding massive black holes (BH) in centers of galaxies [3–5], formed as the BHs grow adiabatically. If DM self-annihilates, the spikes significantly boost the annihilation rate. This has led to searches of bright isolated gamma-ray sources in the sky as well as constraints on DM annihilation cross sections [6–17]. However, the abundance and properties of the DM spikes are uncertain [6,18–22], as the subparsec regions of the BHs can only be probed in a few selected systems [23–25]. Furthermore, there is no guarantee that DM can self-annihilate. This dual uncertainty makes it difficult to constrain either the DM spikes or DM particle properties robustly.

Thankfully, this picture could soon change dramatically. Future space-based gravitational-wave experiments, such as LISA [26], Taiji [27], and TianQin [28] can detect hundreds to thousands of small compact objects falling into massive BHs [29]. These events are called extreme-mass-ratio inspirals (EMRIs). GWs from EMRIs can probe the properties of the surrounding DM spikes [30–34]. By measuring the DM spike profile using purely gravitational interactions, we could reliably detect the spike and simultaneously constrain the DM properties.

Previously, it was demonstrated that EMRI measurements could be used to infer ultralight boson properties [35]. References [36,37] studied the multimessenger prospects for the QCD axion and primordial black hole detection by DM spikes. The potential to test DM properties were also briefly noted in Refs. [2,30,33].

In this work, we show that even with a single GW detection of DM spike, one can place strong constraints on the properties of several popular DM models. These include ultralight bosons, keV fermions, self-annihilating DM, and primordial BHs. We provide the principal arguments and order-of-magnitude, but robust, determination of the constraints.

II. DM SPIKE FORMATION AROUND BHS

Consider massive BHs at the centers of DM halos. The density profile near the BH is approximated by

$$\rho(r) \simeq \rho_0 (r/r_0)^{-\gamma}. \tag{1}$$

*o.hannuksela@nikhef.nl
†c.y.ng@uva.nl
‡tgfli@cuhk.edu.hk

When the BH grows adiabatically, the surrounding DM density evolves into a concentrated "spike" [3,4,38]:

$$\rho_{\rm sp}(r) = \rho_R (1 - 8M_{\rm BH}/r)^3 (r/R_{\rm sp})^{-\alpha}, \tag{2}$$

where $\alpha = (9 - 2\gamma)/(4 - \gamma)$, with $G = c = \hbar = 1$. The factors ρ_R and $R_{\rm sp}$ depend on γ and the BH mass $M_{\rm BH}$ through the M–σ relation as in Ref. [38] and concentration relation from [39]. $\gamma = 1$ corresponds to the NFW profile, and we consider $\gamma = 2$ to be the optimistic case.

Depending on the merger history and the stellar environment of the BHs, the DM spikes could be disrupted and end up with shallower slopes [6,18,40–42]. However, the extent of these effects is debated [12,13], and spikes around lighter BHs are less likely affected by mergers [43,44]. We emphasize that the EMRI GW detection itself does not depend on the formation scenarios or properties of DM (e.g., annihilation).

III. DM SPIKE DETECTION WITH EMRI

Detecting DM spikes: We model GWs from EMRI systems interacting with DM spikes (following Refs. [30,33]), and recover the spike parameters in LISA setting. As the compact objects fall into the BHs, they lose energy and change orbit due to dynamical friction [30,33,45], allowing for a DM spike measurement.

Our setup is as follows: For each BH mass, $M_{\rm BH}$, we set a constant signal-to-noise ratio of SNR = 30 (the usual detection threshold for EMRIs [46]).[1] DM effects are modeled at the lowest post-Newtonian (PN) order for $\rho_{\rm dm}(r) = \rho_{\rm peak}(r/20M_{\rm BH})^{-\alpha}$ profile using stationary phase approximation [47] (see Ref. [33], Supplemental Material). Other binary interactions are at 2.5 PN [48]. We set the mass ratio of the binary $q = \mu/M_{\rm BH} = 10^{-4}$ (our waveform approximation likely breaks down at smaller values of $q \ll 10^{-4}$ and above $q \gtrsim 10^{-3}$ the spike is likely to be destroyed by the inspiraling compact object [49]), and we assume LISA sensitivity with angle-averaged antenna pattern functions [50]. We recover the parameters of the injected waveforms, including $\rho_{\rm peak}$ and the density slope α, by the Fisher information matrix (FIM) method [48,51].[2] We assume 5 years of orbital time and the last orbital cycle at $r = 20M_{\rm BH}$. The choice for the last orbital cycle is motivated by the fact that the DM spike is no longer a power-law below $20M_{\rm BH}$; at a very high radius, the orbit does not shrink, and thus the inspiral does not explore the full profile of the density spike. Note that the latter may not be the case for eccentric orbits, which could explore a larger portion of the spike without losing much of their orbital energy [52]. Generally, larger central black holes allow us to probe to larger distances, and could thus be favored as detection candidates. Systems with very small central black holes may not be detected very far. However, a more detailed EMRI population study will be required to quantify the rate.

[1]Note that the horizon distance, under this assumption, can be very small for light binaries. Our simplistic computation of the optimally oriented SNR indicate that the binaries (as modelled here) can be detected up to $\mathcal{O}(1)$, $\mathcal{O}(100)$ and $\mathcal{O}(1000)$ Mpc for $M = 10^3$, $M = 10^4$ and $M = 10^5$ $\rm M_\odot$ central black hole masses, respectively, depending somewhat on the parameter choice.

[2]We recover $\theta \in \{A, \phi_c, t_c, \log \mathcal{M}_c, \log \eta, \beta, \sigma, \log \rho_{\rm peak}, \alpha\}$, where β, σ represent spin-orbit and spin-spin contributions to the phasing [48].

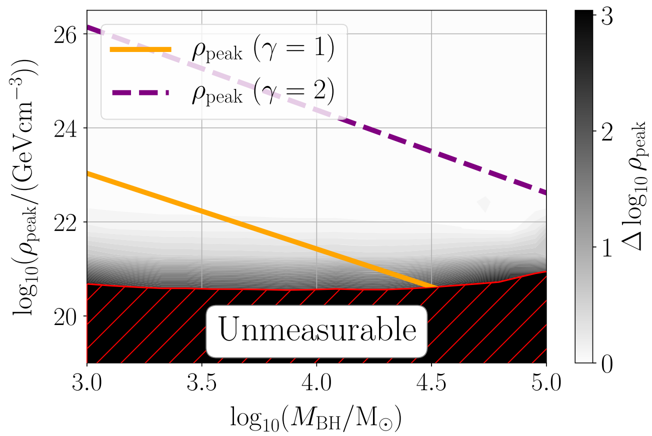

FIG. 1. Uncertainty in the peak DM spike density $\Delta \log_{10} \rho_{\rm peak}$ from EMRI GW measurement around a massive BH as a function of $\rho_{\rm peak}$ and BH mass $M_{\rm BH}$. We set the mass ratio $q = 10^{-4}$ and SNR = 30. Even order-of-magnitude estimates ($\Delta \log_{10} \rho_{\rm max} \lesssim 3$) will be enough to place stringent constraints on the DM models. $\Delta \log_{10} \rho_{\rm max} \lesssim 3$ is satisfied in the range $M_{\rm BH} \in [10^3, 10^{4.5}]$ $M_\odot$ and $M_{\rm BH} \in [10^3, 10^5]$ $M_\odot$ for $\gamma = 1$ and $\gamma = 2$ (thick solid and dashed lines, respectively). Beyond that, we consider the event "unmeasurable."

Figure 1 shows the error on $\rho_{\rm peak}$ recovery. The recovery is accurate ($\Delta \log_{10} \rho_{\rm peak} < 1$) in much of the parameter space. We find $\Delta \log_{10} \rho_{\rm peak} \lesssim 3$ at BH masses $M_{\rm BH} \in [10^3, 10^{4.5}]$ $M_\odot$ and $M_{\rm BH} \in [10^3, 10^5]$ $M_\odot$ for $\gamma = 1$ and $\gamma = 2$, respectively. We consider the cases where $\Delta \log_{10} \rho_{\rm peak} > 3$, as "unmeasurable." At all the considered values, the spike leaves a noticeable orbital shift on the compact object's trajectory. Below 10^3 $M_\odot$, the detector sensitivity deteriorates rapidly [53]. We emphasize that even order-of-magnitude estimates ($\Delta \log_{10} \rho_{\rm peak} \lesssim 3$) can place stringent bounds on the DM models.

We note that at high densities (around the purple line in Fig. 1 and $M \gtrsim 10^{5.5}$ $M_\odot$) the matter-induced phase corrections become larger and the waveform approximation is unsuitable (Ref. [33,35]; Supplemental Material [54]). As the effect is larger, we expect the measurement would be even easier; the measurement precision is thus interpolated from lower density points as a conservative estimate.

More accurate waveforms introduce higher-order effects [55]. In principle, these higher-order corrections could be degenerate with the gravitational drag induced by the spike. However, we expect the degeneracies to be small: the spike introduces a slow cumulative phase shift due to gravitational drag, which is quite distinct from the higher-order effects, such as spin precession.

Our results do not strongly depend on the final spike index, but is most sensitive to $\rho_{\rm peak}$. For simplicity, we fix the SNR and q. A larger SNR would lower the measurable line (by a factor of a few for SNR $= 100$). The gain another factor of few if we choose $q = 10^{-3}$, and vice versa for $q = 10^{-5}$.

Finally, we note that the final DM density index is always $\alpha > 2.25$. If the astrophysical spike disruption effects are important, the slope could be flattened, perhaps ending with a shallow case $\alpha \simeq 1.5$ or an intermediate case $\alpha \simeq 1.8$ [12]. Even in the shallow case, the spike can still be detectable at $\{M_{\rm BH} = 10^3\ M_\odot, \gamma = 2\}$; while in the intermediate case, the spike is detectable at $\{M_{\rm BH} = 10^3\ M_\odot, \gamma \simeq 1.6\}$ or $\{M_{\rm BH} \le 10^4\ M_\odot, \gamma = 2\}$. *The EMRI GW probe can thus be sensitive to a broad range of spike parameters.*

EMRI detection rates: Studies of the expected EMRI rate with self-consistent BH formation and evolution models suggest $\mathcal{O}(100\text{–}1000)$ EMRI observable events in LISA [29]. Importantly, these models favor events with lighter BHs. DM spikes around lighter BHs are denser and thus easier to detect (Fig. 1). Also, light BHs are less likely to suffer from major mergers and thus more likely to retain the DM spikes [30,33,43,44]. DM spikes themselves could *enhance* the merger rates due to dynamical friction effect [56], making them more likely to harbor detectable EMRIs. Here we have fixed our parameter choices for the black hole/DM spike system, and consider somewhat different setup for the rates than considered in, for example, Ref. [29]. Therefore, it is not clear at what rate we would detect the type of system we consider with respect to regular EMRIs. Indeed, a more dedicated study to the EMRI population that explores the whole population of black hole parameters, EMRIs, and DM spikes will be required before we can quantitatively estimate how many DM spikes we might expect to observe with LISA.

IV. DARK MATTER TESTS WITH EMRIS

If DM consists of ultralight bosons, light fermions, self-annihilating particles, or primordial BHs (PBHs), the DM spike density would be affected.

Ultralight bosonic DM: Consider a scalar field ψ_i surrounding the center of a galaxy without a BH. Since the boson is light, it forms a BEC (i.e., it is in ground state; $\psi_i = \psi_i^{\rm ground}$ for some initial Hamiltonian) [57–62]. A BH then grows adiabatically in the center, evolving the surrounding scalar field. The growth takes place on much greater timescale than the scalar field cycle,[3] thus adiabatic theorem [67–69] applies: The final state of the scalar field ψ_f, after growth, will be in the ground state of the final Hamiltonian, which is approximately the BH Hamiltonian near the center [58].

The density of the (final) ground state [63,70]

$$\rho_s(\mu_s, M_{\rm BH}, r, \theta, M_s) \simeq \frac{M_s}{64\pi\mu_s} M_{\rm BH}^5 \mu_s^{11} r^2 e^{-M_{\rm BH}\mu_s^2 r} \sin^2\theta, \quad (3)$$

in the $M_{\rm BH}\mu_s \ll 1$ limit, where μ_s is the boson mass, r is the radius, $M_s = \int \rho r^2 dr d\Omega$ is the cloud mass, and the density has been expanded in leading order of r^{-1}. We assume complex scalar fields, but real fields share similar predictions [64,65,71,72].

The cloud mass must be smaller than the mass inside the influence radius ($M_s \lesssim M_s^{\rm max} \sim 2M_{\rm BH}$ [73]). This translates to constraints on the maximal observed density $\rho_{\rm obs} \lesssim \rho_{\rm max} = \rho_s(\mu, M_{\rm BH}, 2/(M_{\rm BH}\mu_s^2), \pi/2, M_s^{\rm max})$, which yields

$$\mu_s \gtrsim 5 \times 10^{-17}\,{\rm eV} \left(\frac{\rho_{\rm obs}}{10^{20}\,{\rm GeV/cm^3}} \frac{2M_{\rm BH}}{M_s^{\rm max}} \right)^{1/6} \left(\frac{10^5\,M_\odot}{M_{\rm BH}} \right)^{2/3}. \quad (4)$$

Consequently, we could disfavour, e.g., the fuzzy/wave DM candidate in the $\mu_s \in [10^{-23}, 10^{-21}]$ eV range [62,63], proposed as a solution to many cosmological problems (Fig. 2, panel a).

If stars or compact objects of large mass are present near the BH in sufficient abundance, the cloud ground state [Eq. (3)] could mix with higher-order states, or collapse back to the BH [70,77]. In this case, the boson cloud will no longer reside in the ground state, but either does not exist or resides in a higher state. However, higher modes are spread across an even *larger* volume and therefore predict smaller densities [63], making our estimate conservative.

When the boson mass is larger, superradiance can create bosonic clouds [65,66].[4] These clouds may allow one to verify the existence of the bosons by this same EMRI measurement [35] (Fig. 2, panel a, green region, which we show for completeness).

Ultralight bosons could, in principle, inhibit the formation of these tails due to quantum effects [61]. The precise framework to model the gravitational effects by light bosons (or scalar fields) is still worked out [45,74, 78–85]. If light bosons inhibit the tails and thus dynamical friction, then a measurement of the spike implies even *stronger* constraints on the ultralight bosons.

Fermionic DM: Consider a system of a degenerate fermionic DM. The Fermi velocity is

[3]The scalar field oscillation time-scale $\tau \sim \mu_s^{-1} \lesssim 100$ yr $\ll 10^6$ yrs when $\mu_s \gtrsim 10^{25}$ eV [63–66].

[4]In the LISA BH range $M_{\rm BH} \in [10^3, 10^6]\ M_\odot$ would have such "resonant" bosons in the $\mu_s \in [10^{-17}, 10^{-14}]$ eV range.

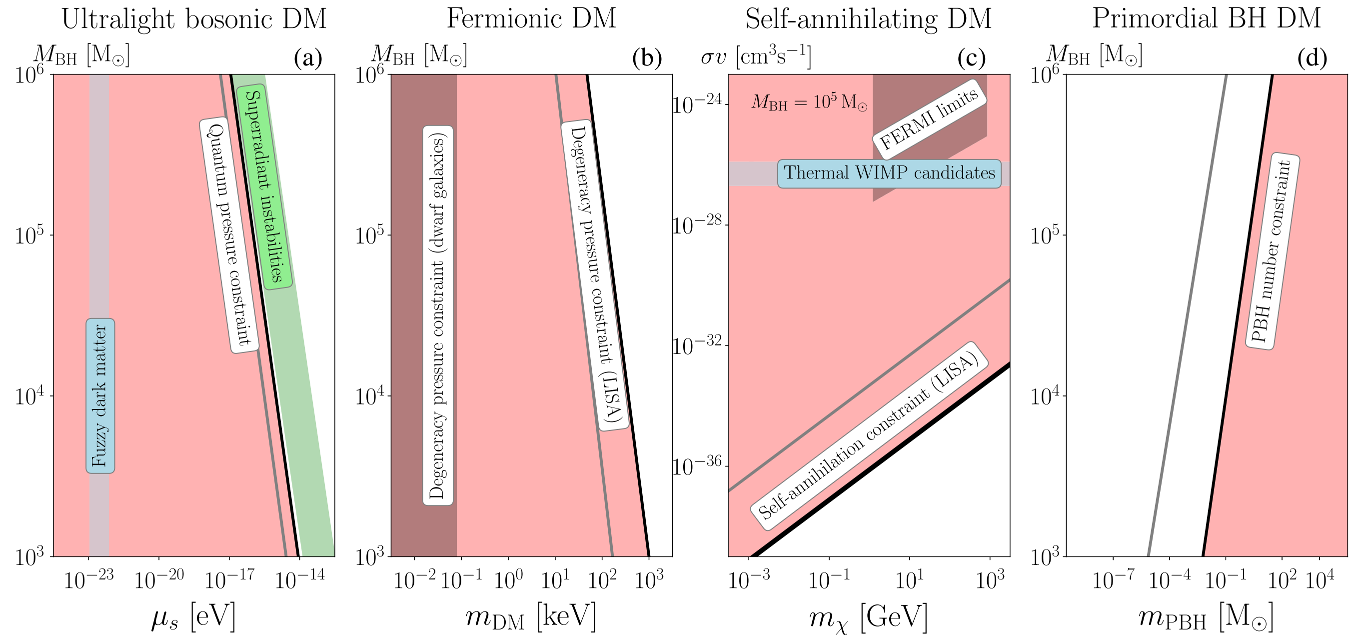

FIG. 2. New constraints (red) on DM models if a DM spike is detected with an EMRI. For ultralight bosons (panel a), fermionic DM (panel b), and PBH DM (panel d), we exclude a region of the DM particle/PBH mass. The constraints depend on the mass of the detected central BH, M_{BH} (the DM spike profile is uniquely predicted for given M_{BH} using the M–σ relation). For self-annihilating DM (panel c), the constraint is on the cross section-DM mass plane, assuming $M_{BH} = 10^5\ M_\odot$. If ultralight bosons exist in the $m_{DM} \in [10^{-17}, 10^{-14}]$ eV range, they could be identified through superradiant-induced clouds (see Ref. [35,70,74]; panel a, green region). Lower limits (gray) on fermionic DM and upper limits on DM annihilation cross section are from Refs. [75,76]. For all panels, the thick solid lines and thin gray lines correspond to $\gamma = 2$ and $\gamma = 1$ initial DM halo slopes, respectively.

$$v_F = \left(\frac{6\pi^2\hbar^3\rho}{m_{DM}^4 g}\right)^{1/3}. \tag{5}$$

For the density spike to be stable, the Fermi velocity must be less than the escape velocity of the BH/DM spike system

$$v_F \leq v_{esc} \equiv \sqrt{\frac{2G(M_{BH} + M_\chi)}{R}} \simeq \sqrt{\frac{2GM_{BH}}{R}}. \tag{6}$$

This translates to a lower bound on the fermionic DM mass, given an observation of density ρ_{obs},

$$m_{DM} \gtrsim 30\,\text{keV}\left(\frac{\rho_{obs}}{10^{20}\ \text{GeV/cm}^3}\frac{2}{g}\right)^{1/4}\left(\frac{R}{20M_{BH}}\right)^{3/8}. \tag{7}$$

Thus, a detection of the DM spike could significantly improve existing fermioninc DM constraint [75] by more than 2 orders of magnitude. While our result only depends on the measured density, we express the constraint in terms of M_{BH} using our reference DM spike model for consistency, as shown in Fig. 2 panel a. This result is robust, and does not depend on the initial phase-space density distribution [86,87]. It will also close the νMSM sterile neutrino DM window [88,89] without relying on X-ray searches [90–97].

Self-annihilating DM: Self-annihilating DM would rapidly smooth out the DM spike, forming an "annihilation plateau" [4]. We approximate the plateau as a flat core, $\rho_{core} = m_\chi/(\sigma v t_{BH})$ [3] (see also [17,42,98]). Taking conservatively the age of the BH to be $t_{BH} \gtrsim 10^6$ years (much less than the age of galaxies or stars, $\sim 10^{10}$ yr), an EMRI DM spike measurement sets an upper limit on the *total* annihilation cross section,

$$\sigma v \lesssim 3.17 \times 10^{-32}\ \text{cm}^3\,\text{s}^{-1}\left(\frac{m_\chi}{100\ \text{GeV}}\right) \times \left(\frac{10^{20}\ \text{GeV/cm}^3}{\rho_{obs}}\right)\left(\frac{10^6\ \text{yr}}{t_{BH}}\right). \tag{8}$$

Thus, any EMRI DM spike measurement will be in strong tension with the simplest thermal relic DM hypothesis (Fig. 2, panel c), currently an open window between 20 GeV $< m_\chi <$ 100 TeV [76]. We emphasize that this is the total cross-section, and thus includes the difficult-to-probe neutrino channels.

For other cases (p-wave annihilation, non-thermal models), the cross-section could be significantly lower [13]. Then, the EMRI event could have a persistent electromagnetic counterpart due to DM annihilation. We find that in the optimistic scenario, where $\gamma = 2$, the BH is heavy $M_{BH} \sim 10^6$ M$_\odot$ (see EMRI detection section, however) and nearby $D \sim 90$ Mpc, the electromagnetic part is detectable by e-ASTROGAM/Fermi/CTA [99–101], by comparing the expected signals with the detector sensitivity, and assuming $\chi\chi \to \tau\tau$ channel [102] (details in Supplemental Material [54]). However, within such a small volume, the expected number of EMRI events is only of order one [103]. Thus, to observe the counterpart, the fraction of halos hosting spikes must be high, the DM spike must be young, and the event must be nearby.

Primordial black hole DM We consider the case that PBHs dominates cosmic DM density. If a DM spike is measured with EMRI, there must be at least one PBH ($N \geq 1$) in the probed volume ($8M_{\mathrm{BH}} < r < 300M_{\mathrm{BH}}$). The mass of the PBH m_{PBH}, must then satisfy

$$m_{\mathrm{PBH}} \leq \int_{8M_{\mathrm{BH}}}^{300M_{\mathrm{BH}}} \rho_{\mathrm{obs}}(r) d^3 r. \tag{9}$$

Consequently, the PBH mass range could be constrained to $m_{\mathrm{PBH}} \lesssim 10^{-7}\ \mathrm{M}_{\odot}$ ($\gamma = 1$, Fig. 2, panel d). This simple PBH number argument offers an independent constraint on the PBHs, complementary to existing considerations (e.g., Refs. [104–109]). We note that the above $N = 1$ constraint is exceptionally conservative. In the case of a spike detection, for the PBH DM to mimic the dynamical friction effect, the spike must have a large amount of PBHs $N \gg 1$, thus leading to more stringent constraints.

One could combine these spike measurements with ground-based detectors that observe PBH mergers within the spikes. However, unfortunately, the fraction of mergers within a single halo is $N_{\mathrm{sp}} \lesssim 10^{-2}\ \mathrm{yr}^{-1}$ [38], and thus constraining PBHs by aid of ground-based detectors would be difficult. We note that PBHs themselves also act as EMRIs, which could offer another channel for their detections [110].

V. DISCUSSION AND CONCLUSION

We have shown that EMRI GW measurement with space interferometry experiments could place strong constraints on DM models across the particle landscape. The EMRI GW emission will provide purely gravitational tests for DM spikes, which is a prediction of cold collisionless DM.

In the DM parameter space we consider here, the DM spike will always flatten due to the intrinsic DM particle properties. On the other hand, astrophysical effects may also partially flatten the spike. A large number of expected EMRIs (∼100–1000) is thus extremely advantageous. They allow us to probe BH systems under various astrophysical conditions and with variable merger histories, reducing the chance of non-detection of the spike due to astrophysical effects. However, a more dedicated study to the EMRI population will be required to make quantitative estimates on the detection rate.

If no spikes are detected, then, unfortunately, no conclusions can be drawn immediately. One possibility is that astrophysical processes (stellar heating, mergers [6,18,21,41]) have destroyed the spikes. The processes must then be common, robust, and applicable to different BHs masses and galaxy properties. Follow-up and detailed astronomical observations of the EMRI events (e.g., [111]) are then necessary to identify the astrophysical mechanism. Indeed, galaxies with large EMRI rates may tend to have stellar cusps, which could negatively bias their likelihood of hosting DM spikes [29,112]. However, a recent work demonstrates that the spikes could *enhance* the merger rates [56].

The properties of DM might also cause the smoothing of the spike. In these cases, the GW observation itself may already contain smoking-gun signatures of the particle DM (e.g., [35]). Otherwise, independent probes are needed to pinpoint the particle effect (gamma-ray searches or others [24,25]).

Here we provide the principal methodologies for DM searches by EMRIs. To fully realize the search potential, realistic waveforms are required. These waveforms should be generic in their ability to model DM distributions. The form of the spike distribution can, in principle, be quite generic. Additionally, the current form of dynamical friction assumes large velocities for the smaller compact object [113]; however, in principle, there will be a dependence on the local DM velocity distribution, which should be quantified. It will also be crucial to study waveforms specialized toward EMRIs [29,114–118]. Indeed, more flexible waveforms should be developed for realistic LISA data analysis. These future studies will be vital to the development of DM spike detection, but we expect the results here to be qualitatively similar in the future.

ACKNOWLEDGMENTS

We thank Emanuele Berti, Richard Brito, Kaze W. K. Wong for their work on a very closely related project, Yifan Wang, for discussion on primordial black holes and Ming-Chung Chu and Po Kin Leung for their supervision on a dark matter spike project. We also thank John F. Beacom for his helpful comments, Richard Brito, for his advice on ultralight bosons, Kaze W. K. Wong, for his remarks on data-analysis, Christopher P. L. Berry for his useful advice on FIM analysis, and Thomas Edwards and Bradley Kavanagh for their comments. O. A. H. is supported by the Hong Kong Ph.D. Fellowship Scheme (HKPFS) issued by the Research Grants Council (RGC) of Hong Kong and by the research program of the Netherlands Organization for Scientific Research (NWO). K. C. Y. N. is supported by a Croucher Fellowship and a Benoziyo Fellowship. T. G. F. L. was partially supported by grants from the Research Grants Council of the Hong Kong (Project No. CUHK14310816, No. CUHK24304317 and No. CUHK14306218), The Croucher Foundation in Hong Kong, and the Research Committee of the Chinese University of Hong Kong.

[1] G. Bertone, D. Hooper, and J. Silk, Particle dark matter: Evidence, candidates and constraints, Phys. Rep. **405**, 279 (2005).
[2] G. Bertone and T. M. P. Tait, A new era in the search for dark matter, Nature (London) **562**, 51 (2018).
[3] P. Gondolo and J. Silk, Dark Matter Annihilation at the Galactic Center, Phys. Rev. Lett. **83**, 1719 (1999).
[4] L. Sadeghian, F. Ferrer, and C. M. Will, Dark-matter distributions around massive black holes: A general relativistic analysis, Phys. Rev. D **88**, 063522 (2013).
[5] F. Ferrer, A. Medeiros da Rosa, and C. M. Will, Dark matter spikes in the vicinity of Kerr black holes, Phys. Rev. D **96**, 083014 (2017).
[6] D. Merritt, M. Milosavljević, L. Verde, and R. Jimenez, Dark Matter Spikes and Annihilation Radiation from the Galactic Center, Phys. Rev. Lett. **88**, 191301 (2002).
[7] F. Aharonian *et al.*, Search for gamma-rays from dark matter annihilations around intermediate mass black holes with the H.E.S.S. experiment, Phys. Rev. D **78**, 072008 (2008).
[8] G. Bertone, M. Fornasa, M. Taoso, and A. R. Zentner, Dark matter annihilation around intermediate mass black holes: An update, New J. Phys. **11**, 105016 (2009).
[9] T. Bringmann, J. Lavalle, and P. Salati, Intermediate Mass Black Holes and Nearby Dark Matter Point Sources: A Myth-Buster, Phys. Rev. Lett. **103**, 161301 (2009).
[10] B. C. Lacki and J. F. Beacom, Primordial black holes as dark matter: Almost all or almost nothing, Astrophys. J. **720**, L67 (2010).
[11] M. Bañados, B. Hassanain, J. Silk, and S. M. West, Emergent flux from particle collisions near a Kerr black hole, Phys. Rev. D **83**, 023004 (2011).
[12] B. D. Fields, S. L. Shapiro, and J. Shelton, Galactic Center Gamma-Ray Excess from Dark Matter Annihilation: Is There A Black Hole Spike?, Phys. Rev. Lett. **113**, 151302 (2014).
[13] J. Shelton, S. L. Shapiro, and B. D. Fields, Black Hole Window Into p-Wave Dark Matter Annihilation, Phys. Rev. Lett. **115**, 231302 (2015).
[14] T. Lacroix, C. Bœhm, and J. Silk, Ruling out thermal dark matter with a black hole induced spiky profile in the M87 galaxy, Phys. Rev. D **92**, 043510 (2015).
[15] M. Wanders, G. Bertone, M. Volonteri, and C. Weniger, No WIMP mini-spikes in dwarf spheroidal galaxies, J. Cosmol. Astropart. Phys. 04 (2015) 004.
[16] P. Sandick, K. Sinha, and T. Yamamoto, Black holes, dark matter spikes, and constraints on simplified models with t-channel mediators, Phys. Rev. D **98**, 035004 (2018).
[17] S. L. Shapiro and J. Shelton, Weak annihilation cusp inside the dark matter spike about a black hole, Phys. Rev. D **93**, 123510 (2016).
[18] P. Ullio, H. S. Zhao, and M. Kamionkowski, A dark-matter spike at the galactic center?, Phys. Rev. D **64**, 043504 (2001).
[19] O. Y. Gnedin, A. V. Kravtsov, A. A. Klypin, and D. Nagai, Response of dark matter halos to condensation of baryons: Cosmological simulations and improved adiabatic contraction model, Astrophys. J. **616**, 16 (2004).
[20] D. Merritt, Evolution of the Dark Matter Distribution at the Galactic Center, Phys. Rev. Lett. **92**, 201304 (2004).
[21] G. Bertone and D. Merritt, Time-dependent models for dark matter at the galactic center, Phys. Rev. D **72**, 103502 (2005).
[22] M. Pato, F. Iocco, and G. Bertone, Dynamical constraints on the dark matter distribution in the milky way, J. Cosmol. Astropart. Phys. 12 (2015) 001.
[23] T. Lacroix, M. Karami, A. E. Broderick, J. Silk, and C. Bœhm, Unique probe of dark matter in the core of m87 with the event horizon telescope, Phys. Rev. D **96**, 063008 (2017).
[24] N. Bar, K. Blum, T. Lacroix, and P. Panci, Looking for ultralight dark matter near supermassive black holes J. Cosmol. Astropart. Phys. 07 (2019) 045.
[25] H. Davoudiasl and P. B. Denton, Ultra light boson dark matter and event horizon telescope observations of M87* (2019).
[26] P. Amaro-Seoane *et al.*, Laser interferometer space antenna, arXiv:1702.00786.
[27] Z.-K. Guo, R.-G. Cai, and Y.-Z. Zhang, *Taiji Program: Gravitational-wave sources* (2018).
[28] J. Luo *et al.*, TianQin: A space-borne gravitational wave detector, Classical Quantum Gravity **33**, 035010 (2016).
[29] S. Babak, J. Gair, A. Sesana, E. Barausse, C. F. Sopuerta, C. P. L. Berry, E. Berti, P. Amaro-Seoane, A. Petiteau, and A. Klein, Science with the space-based interferometer LISA. V: Extreme mass-ratio inspirals, Phys. Rev. D **95**, 103012 (2017).
[30] K. Eda, Y. Itoh, S. Kuroyanagi, and J. Silk, New Probe of Dark-Matter Properties: Gravitational Waves from an Intermediate-Mass Black Hole Embedded in a Dark-Matter Minispike, Phys. Rev. Lett. **110**, 221101 (2013).
[31] E. Barausse, V. Cardoso, and P. Pani, Can environmental effects spoil precision gravitational-wave astrophysics?, Phys. Rev. D **89**, 104059 (2014).
[32] E. Barausse, V. Cardoso, and P. Pani, in *Environmental Effects for Gravitational-Wave Astrophysics*,Journal of Physics: Conference Series, Vol. 610 (IOP Publishing, Florida, USA, 2015), p. 012044.
[33] K. Eda, Y. Itoh, S. Kuroyanagi, and J. Silk, Gravitational waves as a probe of dark matter minispikes, Phys. Rev. D **91**, 044045 (2015).
[34] X.-J. Yue and W.-B. Han, Gravitational waves with dark matter minispikes: The combined effect, Phys. Rev. D **97**, 064003 (2018).
[35] O. A. Hannuksela, K. W. K. Wong, R. Brito, E. Berti, and T. G. F. Li, Probing the existence of ultralight bosons with a single gravitational-wave measurement, Nat. Astron. **3**, 447 (2019).
[36] T. D. P. Edwards, M. Chianese, B. J. Kavanagh, S. M. Nissanke, and C. Weniger, A Unique Multi-Messenger Signal of QCD Axion Dark Matter, Phys. Rev. Lett. **124**, 161101 (2020).
[37] G. Bertone, A. Coogan, D. Gaggero, B. J. Kavanagh, and C. Weniger, Primordial black holes as silver bullets for new physics at the weak scale, Phys. Rev. D **100**, 123013 (2019).
[38] H. Nishikawa, E. D. Kovetz, M. Kamionkowski, and J. Silk, Primordial-black-hole mergers in dark-matter spikes, Phys. Rev. D **99**, 043533 (2019).

[39] M. A. Sánchez-Conde and F. Prada, The flattening of the concentration–mass relation towards low halo masses and its implications for the annihilation signal boost, Mon. Not. R. Astron. Soc. **442**, 2271 (2014).
[40] T. Nakano and J. Makino, On the cusp around central black holes in luminous elliptical galaxies, Astrophys. J. Lett. **525**, L77 (1999).
[41] G. Bertone and D. Merritt, Dark matter dynamics and indirect detection, Mod. Phys. Lett. A **20**, 1021 (2005).
[42] E. Vasiliev and M. Zelnikov, Dark matter dynamics in the galactic center, Phys. Rev. D **78**, 083506 (2008).
[43] H. S. Zhao and J. Silk, Dark Minihalos with Intermediate Mass Black Holes, Phys. Rev. Lett. **95**, 011301 (2005).
[44] G. Bertone, A. R. Zentner, and J. Silk, New signature of dark matter annihilations: Gamma rays from intermediate-mass black holes, Phys. Rev. D **72**, 103517 (2005).
[45] C. F. B. Macedo, P. Pani, V. Cardoso, and L. C. B. Crispino, Into the lair: Gravitational-wave signatures of dark matter, Astrophys. J. **774**, 48 (2013).
[46] J. R. Gair, L. Barack, T. Creighton, C. Cutler, S. L. Larson, E. S. Phinney, and M. Vallisneri, Event rate estimates for lisa extreme mass ratio capture sources, Classical Quantum Gravity **21**, S1595 (2004).
[47] M. Maggiore, *Gravitational Waves. Vol. 1: Theory and Experiments*, Oxford Master Series in Physics (Oxford University Press, New York, 2007).
[48] E. Berti, A. Buonanno, and C. M. Will, Estimating spinning binary parameters and testing alternative theories of gravity with LISA, Phys. Rev. D **71**, 084025 (2005).
[49] B. J. Kavanagh, D. A. Nichols, G. Bertone, and D. Gaggero, Detecting dark matter around black holes with gravitational waves: Effects of dark-matter dynamics on the gravitational waveform, Phys. Rev. D **102**, 083006 (2020).
[50] T. Robson, N. J. Cornish, and C. Liu, The construction and use of LISA sensitivity curves, Classical Quantum Gravity **36**, 105011 (2019).
[51] M. Vallisneri, Use and abuse of the fisher information matrix in the assessment of gravitational-wave parameter-estimation prospects, Phys. Rev. D **77**, 042001 (2008).
[52] A. Nishizawa, E. Berti, A. Klein, and A. Sesana, eLISA eccentricity measurements as tracers of binary black hole formation, Phys. Rev. D **94**, 064020 (2016).
[53] J. R. Gair, S. Babak, A. Sesana, P. Amaro-Seoane, E. Barausse, C. P. L. Berry, E. Berti, and C. Sopuerta, in *Prospects for Observing Extreme-Mass-Ratio Inspirals with Lisa*, Journal of Physics: Conference Series, Vol. 840 (IOP Publishing, Zurich, Switzerland, 2017), p. 012021.
[54] Please see Supplemental Material at http://link.aps.org/supplemental/10.1103/PhysRevD.102.103022 for derivations relating to the dark matter spike profile, parameter estimation, and the adiabatic theorem.
[55] E. Poisson, A. Pound, and I. Vega, The motion of point particles in curved spacetime, Living Rev. Relativity **14**, 7 (2011).
[56] X.-J. Yue, W.-B. Han, and X. Chen, Dark matter: An efficient catalyst for intermediate-mass-ratio-inspiral events, Astrophys. J. **874**, 34 (2019).
[57] W. Hu, R. Barkana, and A. Gruzinov, Fuzzy Cold Dark Matter: The Wave Properties of Ultralight Particles, Phys. Rev. Lett. **85**, 1158 (2000).
[58] L. A. Urena-Lopez and A. R. Liddle, Supermassive black holes in scalar field galaxy halos, Phys. Rev. D **66**, 083005 (2002).
[59] A. P. Lundgren, M. Bondarescu, R. Bondarescu, and J. Balakrishna, Lukewarm dark matter: Bose condensation of ultralight particles, Astrophys. J. Lett. **715**, L35 (2010).
[60] A. Cruz-Osorio, F. S. Guzmán, and F. D. Lora-Clavijo, Scalar field dark matter: Behavior around black holes, J. Cosmol. Astropart. Phys. 06 (**2011**) 029.
[61] H.-Y. Schive, T. Chiueh, and T. Broadhurst, Cosmic structure as the quantum interference of a coherent dark wave, Nat. Phys. **10**, 496 (2014).
[62] J. Zhang, Y.-L.. S. Tsai, J.-L. Kuo, K. Cheung, and M.-C. Chu, Ultralight axion dark matter and its impact on dark halo structure in n-body simulations, Astrophys. J. **853**, 51 (2018).
[63] S. Detweiler, Klein-Gordon equation and rotating black holes, Phys. Rev. D **22**, 2323 (1980).
[64] A. Arvanitaki, S. Dimopoulos, S. Dubovsky, N. Kaloper, and J. March-Russell, String axiverse, Phys. Rev. D **81**, 123530 (2010).
[65] R. Brito, V. Cardoso, and P. Pani, Superradiance, Lect. Notes Phys. **906**, 18 (2015).
[66] R. Brito, V. Cardoso, and P. Pani, Black holes as particle detectors: Evolution of superradiant instabilities, Classical Quantum Gravity **32**, 134001 (2015).
[67] J. J. Sakurai and J. Napolitano, *Modern Quantum Mechanics*, Quantum physics, quantum information and quantum computation (Cambridge University Press, Cambridge, 2017), ISBN 978-0-8053-8291-4, 978-1-108-52742-2.
[68] G. Nenciu, On the adiabatic theorem of quantum mechanics, J. Phys. A **13**, L15 (1980).
[69] A. Mostafazadeh, Adiabatic geometrical phase for scalar fields in a curved spacetime, arXiv:hep-th/9608051.
[70] D. Baumann, H. S. Chia, and R. A. Porto, Probing ultralight bosons with binary black holes, Phys. Rev. D **99**, 044001 (2019).
[71] S.R. Dolan, Instability of the massive Klein-Gordon field on the Kerr spacetime, Phys. Rev. D **76**, 084001 (2007).
[72] A. Arvanitaki, M. Baryakhtar, and X. Huang, Discovering the qcd axion with black holes and gravitational waves, Phys. Rev. D **91**, 084011 (2015).
[73] L. C. Ho, *Coevolution of Black Holes and Galaxies: Volume 1, Carnegie Observatories Astrophysics Series* (Cambridge University Press, 2004).
[74] M. C. Ferreira, C. F. B. Macedo, and V. Cardoso, Orbital fingerprints of ultralight scalar fields around black holes, Phys. Rev. D **96**, 083017 (2017).
[75] C. Di Paolo, F. Nesti, and F. L. Villante, Phase space mass bound for fermionic dark matter from dwarf spheroidal galaxies, Mon. Not. R. Astron. Soc. **475**, 5385 (2018).
[76] R. K. Leane, T. R. Slatyer, John F. Beacom, and K. C. Y. Ng, Gev-scale thermal wimps: Not even slightly dead, Phys. Rev. D **98**, 023016 (2018).

[77] E. Berti, R. Brito, C. F. B. Macedo, G. Raposo, and J. L. Rosa, Ultralight boson cloud depletion in binary systems, Phys. Rev. D **99**, 104039 (2019).
[78] M. Kesden, J. Gair, and M. Kamionkowski, Gravitational-wave signature of an inspiral into a supermassive horizonless object, Phys. Rev. D **71**, 044015 (2005).
[79] R. Becerril, T. Matos, and L. Ureña-López, Geodesics around oscillatons, Gen. Relativ. Gravit. **38**, 633 (2006).
[80] V. Diemer, K. Eilers, B. Hartmann, I. Schaffer, and C. Toma, Geodesic motion in the space-time of a noncompact boson star, Phys. Rev. D **88**, 044025 (2013).
[81] C. F. B. Macedo, P. Pani, V. Cardoso, and L. C. B. Crispino, Astrophysical signatures of boson stars: Quasinormal modes and inspiral resonances, Phys. Rev. D **88**, 064046 (2013).
[82] Y. Brihaye, V. Diemer, and B. Hartmann, Charged q-balls and boson stars and dynamics of charged test particles, Phys. Rev. D **89**, 084048 (2014).
[83] P. Grandclement, C. Somé, and E. Gourgoulhon, Models of rotating boson stars and geodesics around them: New type of orbits, Phys. Rev. D **90**, 024068 (2014).
[84] M. Bošković, F. Duque, M. C. Ferreira, F. S. Miguel, and V. Cardoso, Motion in time-periodic backgrounds with applications to ultralight dark matter halos at galactic centers, Phys. Rev. D **98**, 024037 (2018).
[85] M. C. Ferreira, How do scalar-field dark matter halos react to orbiting bodies?, Phys. Rev. D **99**, 103008 (2019).
[86] S. Tremaine and J. E. Gunn, Dynamical Role of Light Neutral Leptons in Cosmology, Phys. Rev. Lett. **42**, 407 (1979).
[87] S. Horiuchi, P. J. Humphrey, J. Onorbe, K. N. Abazajian, M. Kaplinghat, and S. Garrison-Kimmel, Sterile neutrino dark matter bounds from galaxies of the local group, Phys. Rev. D **89**, 025017 (2014).
[88] L. Canetti, M. Drewes, and M. Shaposhnikov, Sterile Neutrinos as the Origin of Dark and Baryonic Matter, Phys. Rev. Lett. **110**, 061801 (2013).
[89] L. Canetti, M. Drewes, T. Frossard, and M. Shaposhnikov, Dark matter, baryogenesis and neutrino oscillations from right handed neutrinos, Phys. Rev. D **87**, 093006 (2013).
[90] E. Bulbul, M. Markevitch, A. Foster, R. K. Smith, M. Loewenstein, and S. W. Randall, Detection of an unidentified emission line in the stacked x-ray spectrum of galaxy clusters, Astrophys. J. **789**, 13 (2014).
[91] A. Boyarsky, O. Ruchayskiy, D. Iakubovskyi, and J. Franse, Unidentified Line in X-Ray Spectra of the Andromeda Galaxy and Perseus Galaxy Cluster, Phys. Rev. Lett. **113**, 251301 (2014).
[92] K. C. Y. Ng, S. Horiuchi, J. M. Gaskins, M. Smith, and R. Preece, Improved limits on sterile neutrino dark matter using full-sky fermi gamma-ray burst monitor data, Phys. Rev. D **92**, 043503 (2015).
[93] E. G. Speckhard, K. C. Y. Ng, J. F. Beacom, and R. Laha, Dark Matter Velocity Spectroscopy, Phys. Rev. Lett. **116**, 031301 (2016).
[94] D. Powell, R. Laha, K. C. Y. Ng, and T. Abel, Doppler effect on indirect detection of dark matter using dark matter only simulations, Phys. Rev. D **95**, 063012 (2017).
[95] K. Perez, K. C. Y. Ng, J. F. Beacom, C. Hersh, S. Horiuchi, and R. Krivonos, Almost closing the νMSM sterile neutrino dark matter window with NuSTAR, Phys. Rev. D **95**, 123002 (2017).
[96] K. C. Y. Ng, B. M. Roach, K. Perez, J. F. Beacom, S. Horiuchi, R. Krivonos, and D. R. Wik, New constraints on sterile neutrino dark matter from $NuSTAR$ M31 observations, Phys. Rev. D **99**, 083005 (2019).
[97] B. M. Roach, K. C. Y. Ng, K. Perez, J. F. Beacom, S. Horiuchi, R. Krivonos, and D. R. Wik, NuSTAR Tests of sterile-neutrino dark matter: New galactic bulge observations and combined impact, Phys. Rev. D **101**, 103011 (2020).
[98] E. Vasiliev, Dark matter annihilation near a black hole: Plateau versus weak cusp, Phys. Rev. D **76**, 103532 (2007).
[99] M. Tavani *et al.*, Science with e-ASTROGAM: A space mission for MeV–GeV gamma-ray astrophysics, JHEAp **19**, 1 (2018).
[100] http://www.slac.stanford.edu/exp/glast/groups/canda/lat_Performance.htm.
[101] www.cta-observatory.org.
[102] M. Cirelli, G. Corcella, A. Hektor, G. Hutsi, M. Kadastik, P. Panci, M. Raidal, F. Sala, and A. Strumia, PPPC 4 DM ID: A poor particle physicist cookbook for dark matter indirect detection, J. Cosmol. Astropart. Phys. 03 (2011) 051; Erratum, J. Cosmol. Astropart. Phys. 10 (2012) 01.
[103] J. R. Gair, Probing black holes at low redshift using lisa emri observations, Classical Quantum Gravity **26**, 094034 (2009).
[104] F. Capela, M. Pshirkov, and P. Tinyakov, Constraints on primordial black holes as dark matter candidates from capture by neutron stars, Phys. Rev. D **87**, 123524 (2013).
[105] D. Aloni, K. Blum, and R. Flauger, Cosmic microwave background constraints on primordial black hole dark matter, J. Cosmol. Astropart. Phys. 05 (2017) 017.
[106] M. Boudaud and M. Cirelli, Voyager 1 $e^{\pm}$ Further Constrain Primordial Black Holes as Dark Matter, Phys. Rev. Lett. **122**, 041104 (2019).
[107] W. DeRocco and P. W. Graham, Constraining Primordial Black Hole Abundance with the Galactic 511 keV Line, Phys. Rev. Lett. **123**, 251102 (2019).
[108] R. Laha, Primordial Black Holes as a Dark Matter Candidate Are Severely Constrained by the Galactic Center 511 keV γ-Ray Line, Phys. Rev. Lett. **123**, 251101 (2019).
[109] G. Ballesteros, J. Coronado-Blázquez, and D. Gaggero, X-ray and gamma-ray limits on the primordial black hole abundance from Hawking radiation, Phys. Lett. B **808**, 135624 (2020).
[110] F. Kuhnel, A. Matas, G. D. Starkman, and K. Freese, Waves from the centre: Probing pbh and other macroscopic dark matter with lisa, Eur. Phys. J. C **80**, 627 (2020).
[111] K. Akiyama *et al.*, First M87 event horizon telescope results. I. The shadow of the supermassive black hole, Astrophys. J. **875**, L1 (2019).
[112] C. P. L. Berry, S. A. Hughes, C. F. Sopuerta, A. J. K. Chua, A. Heffernan, K. Holley-Bockelmann, D. P. Mihaylov, M. Coleman Miller, and A. Sesana, The unique potential of extreme mass-ratio inspirals for gravitational-wave astronomy, arXiv:1903.03686.

[113] J. Binney and S. Tremaine, *Galactic Dynamics* (Princeton University Press, Princeton, NJ, 2011).

[114] S. Babak, H. Fang, J. R. Gair, K. Glampedakis, and S. A. Hughes, 'Kludge' gravitational waveforms for a test-body orbiting a Kerr black hole, Phys. Rev. D **75**, 024005 (2007); Erratum, Phys. Rev. D **77**, 049902 (2008).

[115] A. J. K. Chua, C. J. Moore, and J. R. Gair, Augmented kludge waveforms for detecting extreme-mass-ratio inspirals, Phys. Rev. D **96**, 044005 (2017).

[116] M. van de Meent, Self-Force Corrections to the Periapsis Advance around a Spinning Black Hole, Phys. Rev. Lett. **118**, 011101 (2017).

[117] M. van de Meent and N. Warburton, Fast self-forced inspirals, Classical Quantum Gravity **35**, 144003 (2018).

[118] A. Antonelli, M. van de Meent, A. Buonanno, J. Steinhoff, and J. Vines, Quasi-circular inspirals and plunges from non-spinning effective-one-body Hamiltonians with gravitational self-force information, Phys. Rev. D **101**, 024024 (2020).